Measuring the Orientability of Shapes

Paul L. Rosin

School of Computer Science, Cardiff University, Cardiff CF24 3AA, Wales, UK
Paul.Rosin@cs.cf.ac.uk

Abstract. An orientability measure determines how orientable a shape is; i.e. how reliable an estimate of its orientation is likely to be. This is valuable since many methods for computing orientation fail for certain shapes. In this paper several existing orientability measures are discussed and several new orientability measures are introduced. The measures are compared and tested on synthetic and real data.

1 Introduction

It is often useful to determine the orientation of a shape. For instance, in robotics to locate a good grasping position. In computer vision, processing is often performed with respect to an object centred and oriented coordinate frame of reference. This can effectively provide descriptions invariant to certain geometric transforms of the object, and speeds up subsequent operations such as matching.

Several schemes exist for estimating the orientation of a shape, but two problems arise. First, some shapes inherently have no well defined orientation – for example a circle. Second, even for shapes with a well defined orientation some methods fail to identify that orientation. This latter limitation applies to the most common method for estimating orientation based on the line which minimises the integral of the squares of distances of the points (belonging to the shape) to the line [10]. This line passes through the centroid of the shape S, and so the squared distance function of interior points to the line at orientation θ is

$$F(\theta) = \iint_S (x \cdot \sin\theta - y \cdot \cos\theta)^2 \; dx\, dy \tag{1}$$

where S has been translated such that its centroid lies on the origin. $F(\theta)$ is minimised when

$$\tan 2\theta = \frac{2\mu_{11}}{\mu_{20} - \mu_{02}} \tag{2}$$

where μ_{pq} are the central moments of order $p+q$. However, under certain conditions, namely

$$\mu_{11} = \mu_{20} - \mu_{02} = 0 \tag{3}$$

$F(\theta)$ is a constant function, and the method fails. Not only does this hold for all n-fold rotationally symmetric shapes with $n > 2$ [12] but also for many more general shapes [11]. This can be demonstrated by constructing some examples.

One way we have constructed a simple polygonal example of such an irregular asymmetric shape is to express the conditions (3) for six vertices using line

W.G. Kropatsch, M. Kampel, and A. Hanbury (Eds.): CAIP 2007, LNCS 4673, pp. 620–627, 2007.

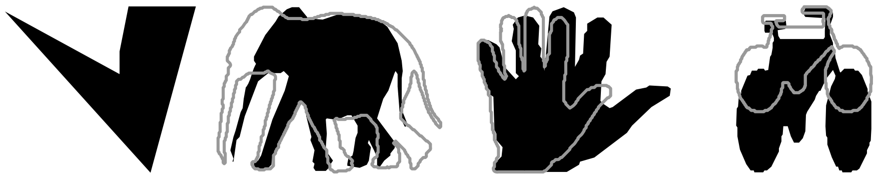

(a) (b) (c) (d)

Fig. 1. Shapes whose orientation is undefined according to the standard method given by (2). The pre-normalised shapes are shown in outline. In all cases $\mu_{11} = \mu_{20} - \mu_{02} = 0$.

moments [9]. After setting coordinate values for four of the vertices the remainder are determined by numerically solving the set of equations. For example, starting with the values $\{(-40, 0), (-40, 100), (0, 300), (300, 300)\}$ yields the remaining values $\{(97.9, -437.2), (-550.6, 277.5)\}$ – see figure 1a.

A more general approach by Süße and Ditrich [11] enables an arbitrary shape to be normalised by a shearing and anisotropic scaling to yield a new shape that satisfies (3) – some examples of such shapes are shown in figure 1b–d.

This limitation of the standard method for orientation estimation has led to the development of methods that can cope in these circumstances. Several are based on higher powers of the distance function $F(\theta)$ and/or higher order moments (including Zernike and generalised complex as well as geometric moments) [8,11,12,14]. Nevertheless, these new orientation estimators are not ideal either, since they may still fail in some cases, and are typically sensitive to noise as a consequence of the higher orders of moments used.

The problems associated with orientation estimation suggest that a measure of *shape orientability*, whose purpose is to describe the degree to which a shape has distinct (but not necessarily unique) orientation, would be useful although there is little previous work in this area [1,16]. Orientability quantifies the likely reliability and stability of orientation estimates. For instance, even minor changes in a shape due to digitization or noise effects can substantially alter orientation estimates for shapes with low orientability [16].

2 Orientability Measures

In this section various schemes (new and old) are described for measuring orientability. There are certain basic properties that we expect all orientability measures to possess (which makes them easier to use and easier to compare):

a) The measured orientability is in the interval $[0, 1]$ for any shape;
b) A circle has the measured orientability equal to 0;
c) The measured orientability is invariant wrt similarity transformations.

In addition, it would be desirable if

d) The only shape with measured orientability equal to 0 is a circle;
e) The only shape with measured orientability equal to 1 is a straight line segment (i.e. the limit of a rectangle as its aspect ratio tends to infinity).

2.1 Moment Based Methods

Elongation. Consider the covariance matrix constructed from the second order central moments of the shape

$$C = \begin{vmatrix} \mu_{20} & \mu_{11} \\ \mu_{11} & \mu_{02} \end{vmatrix}.$$

The eigenvalues of C – denoted by I_1 and I_2 – provide the variances of the shape along the major and minor principal axes. and can be used to form a measure of elongation [5], which in turn is an indication of orientability:

$$\mathcal{D}_F = \frac{I_1 - I_2}{I_1 + I_2} = \frac{\sqrt{4\mu_{11}^2 + (\mu_{20} - \mu_{02})^2}}{\mu_{20} + \mu_{02}} = \frac{\sqrt{\Phi_2}}{\Phi_1}$$

where Φ_1 and Φ_2 are the first two rotation and translation moment invariants [5]. The same measure can be derived from the distance function $F(\theta)$ [16]:

$$\mathcal{D}_F = 1 - \frac{\pi \cdot \min\{F(\theta) \mid \theta \in [0,\pi)\}}{\int_0^\pi F(\theta) \cdot d\theta}.$$

When conditions (3) hold, and consequently $F(\theta)$ is constant, then $\mathcal{D}_F = 0$. Thus, apart from the only true unorientable shape of a circle, the elongation measure underestimates all the other shapes that satisfy (3).

Higher Powers of Distance. One way to correctly determine the orientation of rotationally symmetric shapes is to use higher powers of distance in (1), i.e.

$$F(\theta, p) = \iint_S (x \cdot \sin\theta - y \cdot \cos\theta)^p \ \ dx\, dy.$$

For shapes with N fold rotational symmetry Tsai and Chou [12] used $p = N$, while Žunić *et al.* [14] used $p = 2N$. In a similar manner, a higher order elongation measure can be computed (and thereby an orientability measure). For instance

$$\mathcal{D}_{\mathcal{E}}(p) = 1 - \frac{\min\{F(\theta,p) \mid \theta \in [0, 2\cdot\pi]\}}{\max\{F(\theta,p) \mid \theta \in [0, 2\cdot\pi]\}}$$

is able to distinguish a circular from rotationally symmetric shapes for sufficiently large values of p.

2.2 Geometric Methods

Bounding Rectangles. Žunić *et al.* [16] described a new measure of orientability based on bounding rectangles. For a given shape S let $R(S,\theta)$ be the minimal area rectangle whose edges make an angle θ with the coordinate axes and which includes S and let $\mathbf{A}(R(S,\theta))$ be the area of $R(S,\theta)$. Let

$$\mathbf{A}_{min}(S) \ = \ \min_{\theta\in[0,\pi)} \{ \ \mathbf{A}(R(S,\theta)) \ \} \text{ and } \mathbf{A}_{max}(S) \ = \ \max_{\theta\in[0,\pi)} \{ \ \mathbf{A}(R(S,\theta)) \ \}.$$

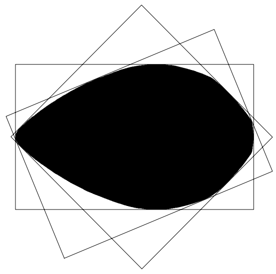

Fig. 2. The minimum area bounding rectangles (three are shown as examples) at all orientations for this shape have constant area but varying aspect ratio; $\mathcal{D}_\alpha = 0$

The orientability of the shape S is defined as:

$$\mathcal{D}_\alpha(S) \; = \; 1 - \frac{\mathbf{A}_{min}(S) - \alpha \cdot \mathbf{A}(S)}{\mathbf{A}_{max}(S) - \alpha \cdot \mathbf{A}(S)}$$

where $\mathbf{A}(S)$ denotes the area of S, and the $\alpha \cdot \mathbf{A}(S)$ terms ($\alpha \in [0,1]$) have been included to enable shapes that have identical convex hulls to be differentiated.

$\mathcal{D}_\alpha$ satisfies the required properties (a), (b) and (c), but not property (d). In fact, $\mathcal{D}_\alpha = 0$ holds not only for the circle, but for all members of the class of curves of constant width (of which the circle is just one instance). The most famous example is the Reuleaux triangle. At all θ the minimum area bounding rectangles $R(S,\theta)$ will be identical squares. Furthermore, it is also possible to have other shapes with varying width that nevertheless have $\mathcal{D}_\alpha = 0$. In such cases the aspect ratio of $R(S,\theta)$ varies over θ, but $\mathbf{A}(R(S,\theta))$ remains constant, as shown in figure 2.

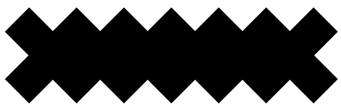

Fig. 3. This shape has orientability $\mathcal{D}_P = 0$

Projection of Edges. In place of (2) Žunić [13] suggested computing the orientation that maximises the squared projection of the shape's boundary. If the edges in polygon P have angles θ_i and lengths l_i, $i = 1 \ldots n$, with respect to the x-axis, then the required orientation θ_0 can be found as

$$\tan 2\theta_0 = \frac{\sum_{i=1}^{n} l_i^2 \, \sin 2\theta_i}{\sum_{i=1}^{n} l_i^2 \, \cos 2\theta_i}.$$

We then compute orientability using the squared projection values at θ_0 and $\theta_0 + \frac{\pi}{2}$ as

$$\mathcal{D}_P = 1 - \frac{\sum_{i=1}^{n} l_i^2 \, \sin(\theta_i - \theta_0)}{\sum_{i=1}^{n} l_i^2 \, \cos(\theta_i - \theta_0)}. \tag{4}$$

A problem with this approach is that it can give unexpected results in some instances, see for example figure 3 which has $\mathcal{D}_P = 0$ since the edge angles are distributed evenly in two orthogonal directions like a square. Given the measure's sensitivity to local deviations in edge orientations, if the boundary is extracted from an image then it needs to have simplification (polygonal approximation) applied to eliminate these variations.

However, this leads to another problem: variations in the sampling rate. For instance, consider an elongated rectangle from which points are selected along the boundary. Sampling at regular intervals will produce a high value of $\mathcal{D}_P$. However, the value of $\mathcal{D}_P$ can be arbitrarily reduced by sampling the long side more densely than the short side. Since the projected lengths are squared then the effect in (4) of the segments from the long side will decrease.

A solution to both these problems can be found in a technique previously employed for measuring rectilinearity [7]. The original data rather than its polygonal approximation is used, but is smoothed over a range of scales. The maximum orientability over scale is then selected. If a curve is smoothed using the geometric heat flow equation then it becomes more and more circular, eventually shrinking to a circular point in finite time [3]. Thus blurring will not increase orientability unless it reveals an elongated global structure that was effectively masked from the measure $\mathcal{D}_P$ by local edges whose orientations are not aligned with the global structure.

Weighting of Edges. Duchêne *et al.* [1] describe a method for estimating orientation which also includes a confidence factor which can be used as an orientability measure. Orientations are considered for $\theta \in [0, \pi)$. The absolute difference in orientation ϕ_i of each edge from θ is taken modulo π. For each edge, if $\phi_i < \delta$ then it contributes the following weight $w_i = l_i(1 - \frac{\phi_i}{\delta})$. Orientation is taken as the value of θ maximising $\sum_{i=1}^{n} w_i$. The same process is carried out to compute orientability as

$$\mathcal{D}_W = \max_{\theta \in [0, \frac{\pi}{2})} \frac{\sum_{i=1}^{n} w_i}{\mathrm{perim}(P)}$$

except that ϕ_i are now taken modulo $\frac{\pi}{2}$.

Note that if $\delta = \frac{\pi}{n}$ then the measure is over the interval $\left(\frac{2}{n}, 1\right]$ rather than $[0, 1)$. Duchêne *et al.* set $\delta = \frac{\pi}{12}$, and in our experiments we have done likewise.

Circularity Measures. Since a circle should produce an extreme value of orientability it seems reasonable that some of the measures of circularity can be used to measure orientability. Let the circumscribed circle, inscribed (i.e. largest empty) circle and convex hull of polygon P be denoted by $\mathrm{CC}(P)$, $\mathrm{IC}(P)$ and $\mathrm{CH}(P)$. These geometric constructions are robust with respect to perturbations of the boundary which makes them suitable for use as elements of shape descriptors. Moreover, the inscribed circle can be computed in $O(n \log n)$ time [6] and the other two can be computed in linear time [2,4]. Note that $\mathrm{IC}(P) \leq \mathrm{CH}(P) \leq \mathrm{CC}(P)$.

Only for the least orientable shape – a circle – does $\mathrm{CC}(P) = \mathrm{IC}(P) = \mathrm{CH}(P)$, and so they can be simply combined to form the following orientability measures, which can be based on either area or perimeter values:

$$\mathcal{C}_1 = 1 - \frac{\mathrm{area}(\mathrm{CH}(P))}{\mathrm{area}(\mathrm{CC}(P))}; \qquad \mathcal{C}_2 = 1 - \frac{\mathrm{area}(\mathrm{IC}(P))}{\mathrm{area}(\mathrm{CH}(P))};$$
$$\mathcal{C}_3 = 1 - \frac{\pi}{\pi-2}\left(\frac{\mathrm{perim}(\mathrm{CH}(P))}{\mathrm{perim}(\mathrm{CC}(P))} - \frac{2}{\pi}\right); \mathcal{C}_4 = 1 - \frac{\mathrm{perim}(\mathrm{IC}(P))}{\mathrm{perim}(\mathrm{CH}(P))}.$$

Incorporating the circumscribed circle in the measure will ensure that protrusions are counted against circularity (and therefore in favour of orientability) while the inscribed circle will ensure that intrusions are treated likewise: counted against circularity and in favour of orientability. Further possibilities are also possible, using for instance linear combinations of the above such as $\alpha\mathcal{C}_1 + (1-\alpha)\mathcal{C}_2$ or different scale normalisations (e.g. using polygon diameter).

3 Experiments

To visualise the similarities and differences between the various orientability measures they have been applied to order some simple shapes as shown in figure 4. Overall we can see that the circle is always assigned a low orientability score while the rectangle receives a high score, but there are many differences in behaviour for intermediate shapes.

As expected, the low order moments measure $\mathcal{D}_F$ is unable to discriminate between the rotationally symmetric shapes which all are assigned a value close to zero (the difference from zero being due to numerical and digitisation errors). In addition, two shapes – the rippled pear and the donkey – have been normalised according to Süße and Ditrich's scheme [11], and consequently also have approximately zero values. Using higher order powers overcomes this problem, as seen in the ranking by $\mathcal{D}_{\mathcal{E}}(50)$. Since this is still effectively an area based measure then small area features, such as the indentation in the circle (second shape from left), have little effect.

As explained in section 2.2 $\mathcal{D}_\alpha$ has a problem with certain shapes such as the irregular Reuleaux shape, fourth from the left for $\mathcal{D}_{\alpha=0.0}$, and the third shape from the left, also described in figure 2. The effect of increasing the value of α is demonstrated: the circle and rectangle have identical values to their modified version with deep intrusions at $\alpha = 0$, but are increasingly discriminated as α increases. Note however that $\mathcal{D}_{\alpha=1.0}$ assigns a square the same peak value of one as a rectangle since $\mathbf{A}_{min} = \mathbf{A}$.

Putting the edge projection method in a multi-scale context ($\mathcal{D}_P$) enables it to successfully cope with the zigzag rectangle (second on the right). Also, being boundary based it is very sensitive to the deep (but narrow) indentations which make the modified circle and rectangle much more orientable. It also discriminates between the plain square and the modified version with the zigzag pattern on the top and bottom, but fails however to distinguish between a square, cross and a circle.

As mentioned previously, Duchêne *et al.*'s method [1] ($\mathcal{D}_W$) does not reach the lower bound of zero, even for a circle. Another point to note is that all the

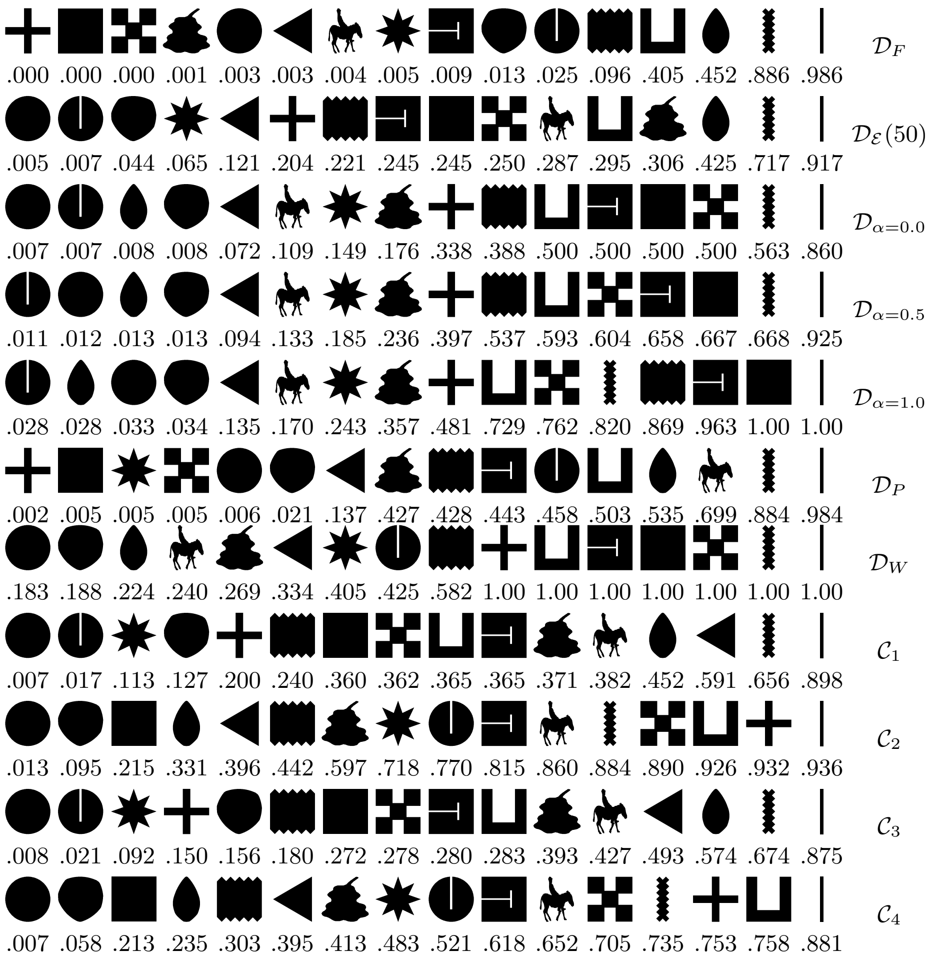

Fig. 4. Shapes ranked according to various orientability measures

rectilinear shapes achieve a value of one, suggesting that this is actually more of a rectilinearity measure [15,7] rather than an orientability measure.

The circularity measures that incorporate the inscribed circle ($\mathcal{C}_2, \mathcal{C}_4$) are more sensitive to intrusions that the remaining circularity measures, which makes the modified circle and rectangle more orientable. At least in these examples there does not appear to be a significant difference between the area and perimeter based versions.

Note that several measures cannot distinguish the 'U' shape from a square: $\mathcal{D}_{\alpha=0.0}$, $\mathcal{D}_W$, $\mathcal{C}_1$, $\mathcal{C}_3$. Also, the shapes are more clearly ordered by some measures; e.g. half the shapes have almost identical $\mathcal{D}_F$ values. Quantifying this for each measure by the median of the differences in the ordered values gives $\{.004, .024, .037, .051, .049, .015, .016, .040, .046, .058, .051\}$, confirming that $\mathcal{D}_{\alpha>0}$ and the circularity measures perform well in this respect.

4 Conclusions

Several orientability measures have been described and tested. While they all operate successfully for extremes of orientability – i.e. a circle and an elongated rectangle – performance is varied for intermediate shapes. Many of the measures cannot distinguish between dissimilar shapes, e.g. the class of rotationally symmetric shapes, constant width shapes, or squares versus circles. Future work will look at applying the orientability measures as shape descriptors, and evaluating their effectiveness for various object classification tasks.

References

1. Duchêne, C., Bard, S., Barillot, X., Ruas, A., Trévisan, J., Holzapfel, F.: Quantitative and qualitative description of building orientation. In: Workshop on Progress in Automated Map Generalisation (2003)
2. Gärtner, B.: Fast and robust smallest enclosing balls. In: Nešetřil, J. (ed.) ESA 1999. LNCS, vol. 1643, pp. 325–338. Springer, Heidelberg (1999)
3. Grayson, M.A.: The heat equation shrinks embedded plane curves to round points. Journal of Differential Geometry 26, 285–314 (1987)
4. McCallum, D., Avis, D.: A linear algorithm for finding the convex hull of a simple polygon. Inform. Process. Lett. 9, 201–206 (1979)
5. Mukundan, R., Ramakrishnan, K.R.: Moment Functions in Image Analysis – Theory and Applications. World Scientific, Singapore (1998)
6. Preparata, F.P., Shamos, M.I.: Computational Geometry. Springer, Heidelberg (1985)
7. Rosin, P.L., Žunić, J.: Measuring rectilinearity. Computer Vision and Image Understanding 99(2), 175–188 (2005)
8. Shen, D., Ip, H.H.S.: Optimal axes for defining the orientations of shapes. Electronic Letters 32(20), 1873–1874 (1996)
9. Singer, M.H.: A general approach to moment calculation for polygons and line segments. Pattern Recognition 26(7), 1019–1028 (1993)
10. Sonka, M., Hlavac, V., Boyle, R.: Image Processing, Analysis, and Machine Vision. PWS (1998)
11. Süße, H., Ditrich, F.: Robust determination of rotation-angles for closed regions using moments. In: Int. Conf. Image Processing, vol. 1, pp. 337–340 (2005)
12. Tsai, W.H., Chou, S.L.: Detection of generalized principal axes in rotationally symetric shapes. Pattern Recognition 24(1), 95–104 (1991)
13. Žunić, J.: Boundary based orientation of polygonal shapes. In: Chang, L.-W., Lie, W.-N. (eds.) PSIVT 2006. LNCS, vol. 4319, pp. 108–117. Springer, Heidelberg (2006)
14. Žunić, J., Kopanja, L., Fieldsend, J.E.: Notes on shape orientation where the standard method does not work. Pattern Recognition 39(5), 856–865 (2006)
15. Žunić, J., Rosin, P.L.: Rectilinearity measurements for polygons. IEEE Trans. on Patt. Anal. and Mach. Intell. 25(9), 1193–1200 (2003)
16. Žunić, J., Rosin, P.L., Kopanja, L.: On the orientability of shapes. IEEE Trans. on Image Processing 15(11), 3478–3487 (2006)